Cilt 11, Sayı 1, Sayfa 95-101, 2022 Volume 11, Issue 1, Page 95-101, 2022

Araştırma Makalesi https://doi.org/10.46810/tdfd.1011220 Research Article

Türk Doğa ve Fen Dergisi
Turkish Journal of Nature and Science
www.dergipark.gov.tr/tdfd

Synthesis and Characterization of ZnO@Fe3O4 Composite Nanostructures by Using Hydrothermal Synthesis Method

Naim ASLAN[1*]

[1]Munzur University, Faculty of Engineering, Department of Metallurgical and Materials Engineering, Tunceli, Turkey
Naim ASLAN ORCID No: 0000-0002-1159-1673

**Corresponding author: aslan.naim@gmail.com; naimaslan@munzur.edu.tr*

(Received: 18.10.2021, Accepted: 08.03.2022, Online Publication: 25.03.2022)

Keywords
Nanocomposite, $ZnO@Fe_3O_4$, Morpho-structural characteriza-tion, Medical imaging, Magnetic and optical properties

Abstract: In this study, $ZnO@Fe_3O_4$ composite nanostructures were synthesized using the hydrothermal method. X-ray diffraction analysis was performed for the structural characterization of nanostructures obtained with the addition of Fe_3O_4 at different ratios, and no impurity peaks were found. Scanning electron microscope (SEM) and transmission electron microscope (TEM) were used for morphological imaging. It was understood that ZnO nanoparticles were decorated around Fe_3O_4 in the morphology of nanostructures. Fe, Zn, and O peaks were detected in elemental analysis. Energy band gaps of $ZnO@Fe_3O_4$ nanocomposite structures were obtained from absorbance data collected by use of UV-VIS spectrometer. The band gap values of nanostructures were calculated to be in the range of 2-2.1 eV. Magnetic properties were determined using a vibrating sample magnetometer (VSM), and the values of 3.76 emu/g and 7.96 emu/g were found depending on the Fe_3O_4 content. Although these values show a limited ferromagnetic property, they are important in optoelectronic and medical imaging applications due to the advanced optical and electronic properties of ZnO.

Hidrotermal yöntem kullanılarak ZnO@Fe3O4 kompozit nanoyapıların sentezi ve karakterizasyonu

Anahtar Kelimeler
Nanokompozit $ZnO@Fe_3O_4$, Morfo-yapısal karakterizas-yon, Medikal görüntüleme, Manyetik ve optik özellikler

Öz: Bu çalışmada, $ZnO@Fe_3O_4$ kompozit nanoyapılar hidrotermal yöntem kullanılarak sentezlenmiştir. Farklı oranlarda Fe_3O_4 katkısıyla elde edilen nanoyapıların yapısal karakterizasyonu için X-ışını kırınım analizi gerçekleştirildi ve herhangi bir safsızlık pikine rastlanmadı. Morfolojik görüntülemede taramalı elektron mikroskobu (SEM) ve geçirimli elektron mikroskobu (TEM) kullanıldı. Nanoyapıların morfolojisinde Fe_3O_4 etrafında ZnO nano taneciklerinin dekore edildiği anlaşılmıştır. Elemental analizde ise Fe, Zn ve O pikleri kaydedilmiştir. $ZnO@Fe_3O_4$ nanokompozit yapıların bant aralığı enerjileri Uv-Vis spektromotresi aracığılıyla elde edilen absorbans datalarından elde edilmiştir. Nanoyapıların bant gap değerleri yaklaşık olarak 2-2.1 eV aralığında hesaplanmıştır. Manyetik özellikler ise Vibrating Sample Magnetometer (VSM) kullanılarak tespit edildi ve Fe_3O_4 katkı oranına bağlı olarak 3.76 emu/g ile 7.96 emu/g değerleri bulundu. Bu değerler sınırlı bir ferromanyetik özellik göstermesine rağmen ZnO'nun sahip olduğu gelişmiş optik, elektronik özelliklerinden dolayı optoelektronik ve medikal görüntüleme uygulamalarında önem arz etmektedir.

1. INTRODUCTION

Nanostructures, which are the basic elements of nanoscience and nanotechnology, have come to the fore as important engineering materials in composite, semiconductor, photocatalytic, magnetic, metal oxide, and biomedical applications with their structural, physical, chemical, and biological properties. Metallic-based nanostructures have received intense attention from both scientific and industrial community [1]. As a matter of fact, magnetic information storage has gained a place in a wide range of areas from industrial applications such as biomedicine and catalysis to new applications in photonics, imaging, and biomedical field [2]. Metallic or metal oxide nanostructures have been extensively studied in recent years due to their specific surface area and crystallinity. Metallic nanostructures stand out in technological product developments with their tunable and improvable properties such as melting

points, electrical and thermal conductivity, light absorption and scattering properties, optical sensitivity, photocatalytic activity, and wettability. Zinc oxide (ZnO), which is a metal oxide, is a biocompatible metal oxide resistant to corrosion and oxidation with its cheap raw material, high crystallinity, synthesis at low temperatures, high optical transmittance, and electrical conductivity. With these significant properties, it has become an important engineering material for optoelectronics, solar cells, detectors, biosensors, drug delivery, and biomedical applications [3]. Iron-based magnetic nanoparticles, especially Fe_3O_4 as another important metal oxide, are important materials used in ceramics, catalysis, magnetic information storage, medical imaging, drug delivery, biomedical applications, and various electronic applications with their natural magnetic properties. Thus, thanks to the unique and compatible properties of their structures, Fe_3O_4 and ZnO allow the production of a higher performance hybrid or composite nanostructure in future applications. In previous studies, sol-gel [4, 5], co-precipitation [6], deposition [7], wet milling [8], microwave assisted [9], and wet chemical [10] methods were used for the synthesis of ZnO/Fe_3O_4 nanocomposites.

ZnO based nanostructures show good electric, optoelectronic, and catalytic properties [11-13]. Fe_3O_4 nanoparticles illustrates superparamagnetic and/or ferromagnetic properties depending on their size [14]. Decorating ZnO nanoparticles with Fe_3O_4 give them magnetic characteristics which enhance the application range of the ZnO nanoparticles [6,10]. Therefore, particles electrical and electronically active ZnO nanoparticles with good magnetic properties can be used in different applications such as magnetic filtering, magnetic catalysis materials, etc [15]. Recently, the hydrothermal method has started to be used for producing nanosized hybrid materials. This method allows the synthesis of different hybrid structures under suitable pressure and temperature conditions without disturbing the chemical structure of the materials [16]. In the present study, the structural, morphological, optoelectronic, and magnetic properties of ZnO@Fe_3O_4 nanostructures obtained in different ratios (1:1 and 1:2) using the hydrothermal method were investigated in detail. SEM (scanning electron microscopy) and TEM (transmission electron microscopy) were used in the structural analysis. EDS (energy dispersive spectra) and X-ray diffraction methods were used in the analysis of chemical composition. UV-vis spectroscopy was used to assess the energy band gaps. Vibrational sample magnetometry was used in the investigation of the magnetic characteristics.

2. MATERIALS AND METHODS

2.1. Materials and Measurements

Iron(II) sulfate ($FeSO_4 \cdot 7H_2O$, Sigma-Aldrich), zinc acetate ($Zn(CH_3CO_2)_2.2H_2O$, Sigma-Aldrich) salts, and urea ($CO(NH_2)_2$, Sigma-Aldrich, PEG (polyethylene glycol; MW=4,000), NaOH (sodium hydroxide) were used for the synthesis of ZnO@Fe_3O_4 nanostructures. X-ray diffraction (XRD) patterns (RIGAKU miniflex600), scanning electron microscope (SEM-HitachiSU3500), high resolution transmission electron microscopy (HR-TEM, Joel 2100 F), energy dispersive x-ray spectroscopy (EDS, Oxford), UV-Vis spectrum (UV-1800 ENG240V), and vibrating sample magnetometer (Cryogenic Limited PPMS) were used for structural, morphological, elemental, optical, and magnetic characterizations, respectively.

2.2. Synthesis of ZnO Nanoparticles

After 1 g of PEG was dissolved in 20 mL of water, 2.19 g of $Zn(CH_3CO_2)_2.2H_2O$ salt was added. After dissolution, 0.5 M 20 mL urea solution was added dropwise. The resulting mixture was transferred to 50 mL capacity Teflon lined stainless steel autoclaves and then heated in an oven at 150 ºC for 12 hours. After spontaneous cooling to room temperature, the precipitate was rinsed with distilled water and ethanol and dried at 80 ºC for 12 hours. The resulting solid was annealed in a muffle furnace at 350 ºC for 2 hours (with a temperature increase of 2 ºC/min).

2.3. Synthesis of Magnetic ZnO@Fe_3O_4 Composite Nanostructures

0.2 g of ZnO was dispersed in 20 mL of deionized water in an ultrasonic bath. In a separate beaker, 0.328 g of $FeSO_4.7H_2O$ was dissolved in 20 mL of deionized water. 1.6 g of NaOH was added to it, and it was mixed for 10 minutes. Then the prepared solution was poured onto ZnO. It was mixed in the ultrasonic bath for 5 more minutes, taken to 50 mL capacity Teflon autoclave coated with stainless steel, and kept at 150 ºC for 12 hours. The resulting black precipitate was collected by centrifugation at 8000 rpm for 20 minutes by use of a centrifuge and washed with deionized water and absolute ethanol several times. The precipitate was kept at 80 ºC for 12 hours (ZnO@Fe_3O_4-1:1). The same procedures were repeated for 0.656 g of $Fe_3O_4.7H_2O$ and 3.2 g of NaOH (ZnO@Fe_3O_4-1:2) [17-19]. Also, such process are illustrated schematically in Fig. 1.

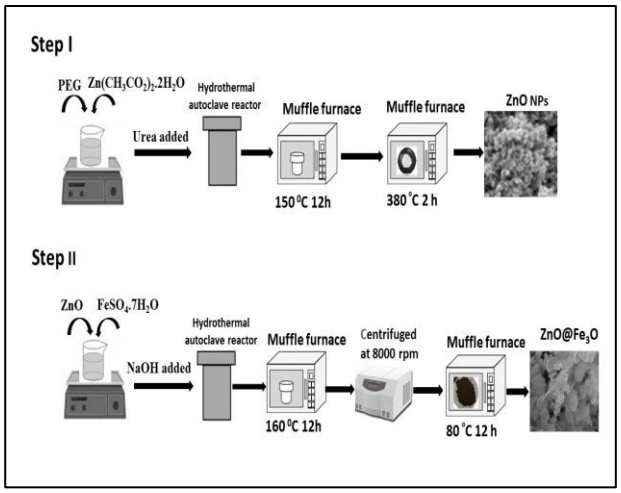

Figure 1. Schematic representation of synthesized ZnO@Fe_3O_4 nanostructures using hydrothermal method

3. RESULTS AND DISCUSSION

3.1. Morpho-structural Characteristic of Nanostructures

The XRD graph of ZnO, Fe_3O_4, ZnO@Fe_3O_4 (1:1), and ZnO@Fe_3O_4 (1:2) nanostructures synthesized by the hydrothermal method is given in Figure 2. As can be understood from the XRD diffraction patterns obtained, peaks characteristic to the ZnO and Fe_3O_4 structures were also observed in ZnO@Fe_3O_4 nanostructures with 1:1 and 1:2 weight ratios. In the ZnO@Fe_3O_4 (1:2) diffraction, the characteristic peaks became more evident with the increase of Fe_3O_4 content. However, the ZnO peak intensity decreased. In addition, the lack of any impurity peak in the XRD diffraction patterns in these structures indicates that they have high crystallinity. The resulting XRD patterns were seen to be consistent with the ZnO@Fe_3O_4 nanostructures obtained by different methods in the literature, but they gave better results in terms of impurity [5,6], [20-22].

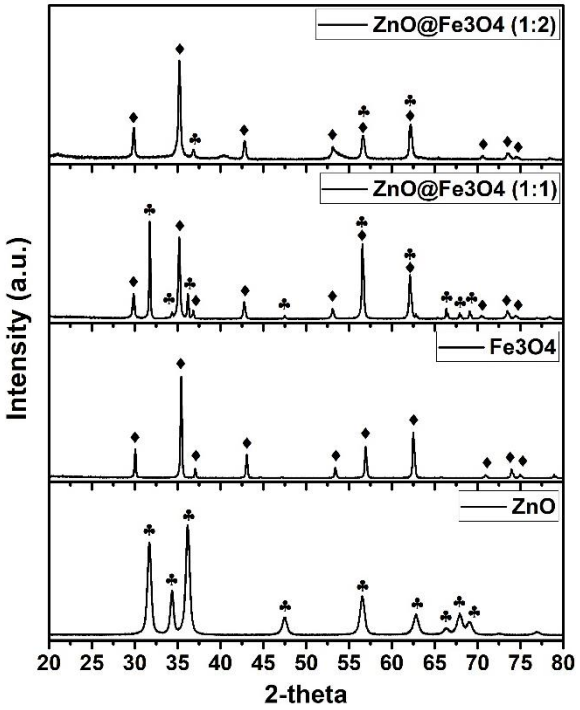

Figure 2. XRD spectra of ZnO, Fe_3O_4, and ZnO@Fe_3O_4 nanostructures

The synthesized SEM images of the ZnO nanostructures containing different weight ratios of Fe_3O_4 are shown in Figure 3a and Figure 3b. As shown in the SEM images, the ZnO and Fe_3O_4 structures were detected to have composite character. In addition, TEM analysis was carried out to check the nano dimensions of the composite structures. The presence of different types of structures was observed in the TEM analysis, as shown in Figure 4a and Figure 4b. It was understood that 10-20 nm irregular spherical ZnO NPs accumulated around Fe_3O_4 structures with 50-100 nm amorphous branches [22].

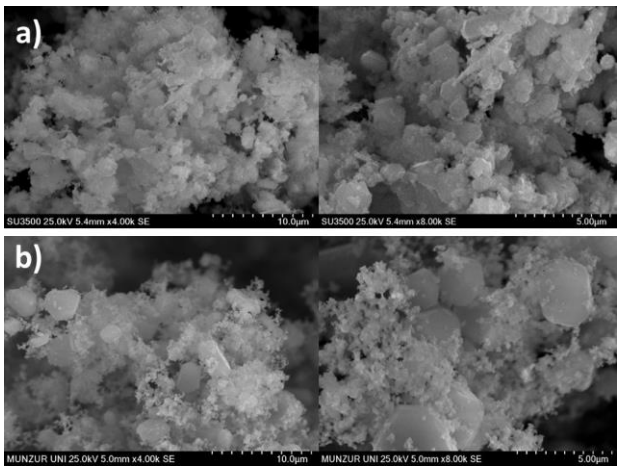

Figure 3. SEM photos of ZnO@Fe3O4 (1:1), ZnO@Fe3O4 (1:2)

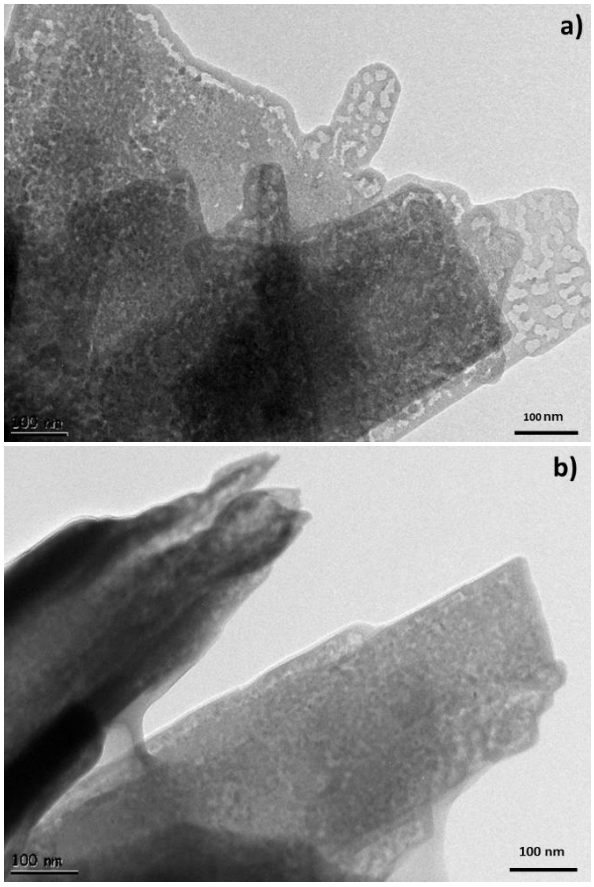

Figure 4. TEM photos of (a)-ZnO@Fe_3O_4(1:1), (b)-ZnO@Fe_3O_4 (1:2)

The EDS-spot and EDS-mapping results of the hydrothermally synthesized ZnO@Fe_3O_4 nanostructures are shown in Fig. 5 and Fig. 6, respectively. Fe, Zn, O were observed in the obtained EDS spectrum as shown in Figure 5a and Figure 5b. Before the SEM investigations Au sputtering was applied to the samples which is a standard procedure used to enhance the performance of the SEM. This is procedure cause a visible Au peak in the EDS spectra. Such a peak is not related to the structure of the nanoparticles. While the percentages of the Fe, Zn, and O elements in the ZnO@Fe_3O_4 (1:1) nanostructure were 38.9, 35.4, and 23.5, respectively, they were observed as 62.7, 16.8, and 19.4 in the ZnO@Fe_3O_4 (1:2) nanostructure. Addition of Fe_3O_4 at different weight ratios nearly doubled the Fe

ratio in the structure. Moreover, in the EDS-mapping images given in Figure 6a and 6b, color intensities are presented based on the presence and content of the Fe, Zn, and O phases in the ZnO@Fe_3O_4 composite structure.

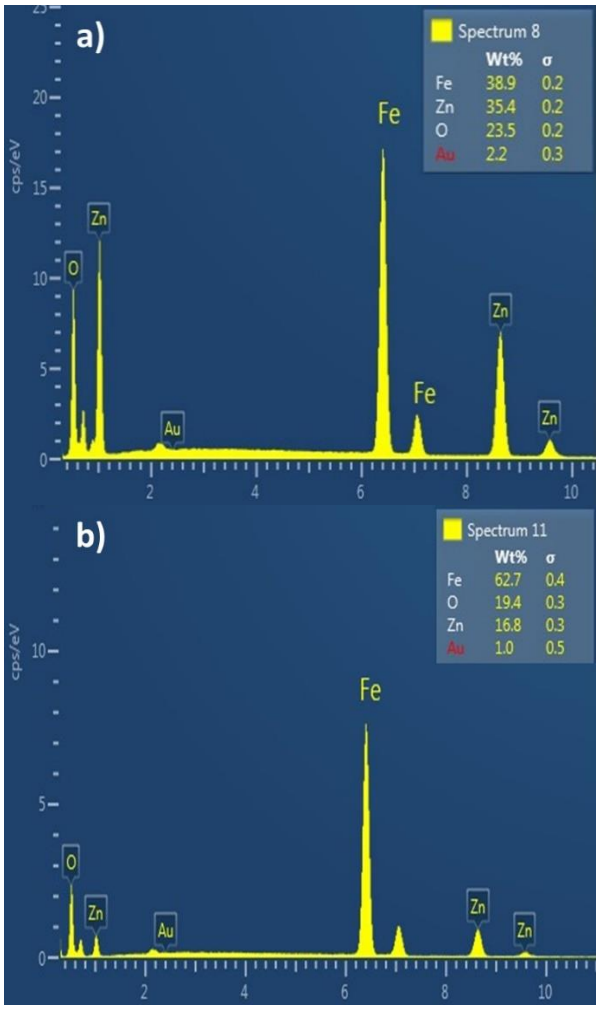

Figure 5. EDS spectrum of (a)-ZnO@Fe_3O_4 (1:1), (b)-ZnO@Fe_3O_4 (1:2)

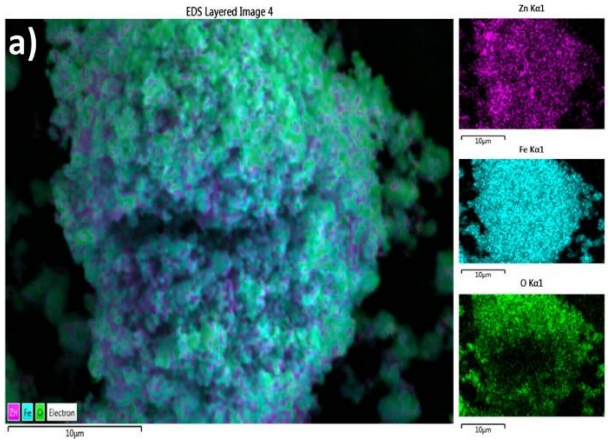

Figure 6. (a) EDS-mapping spectrum of (a)-ZnO@Fe_3O_4(1:1) nanostructure

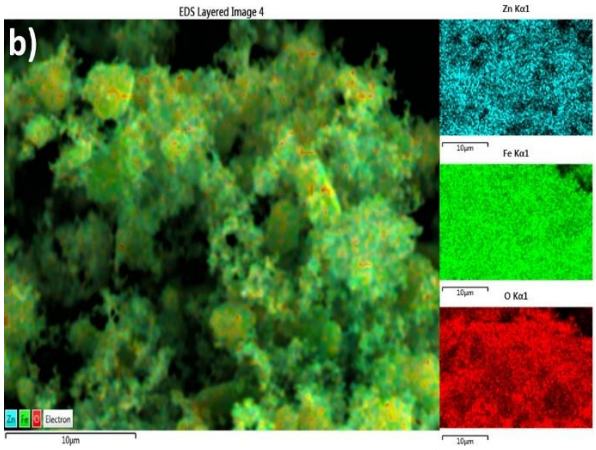

Figure 6. (b) EDS-mapping spectrum of) ZnO@Fe_3O_4(1:2) nanostructure

3.2. Optical Properties of ZnO@Fe_3O_4 Nanostructures

The optical absorbance data of the hydrothermally produced ZnO, Fe_3O_4, and ZnO@Fe_3O_4 nanostructures scanned in the range of 200 nm-800 nm are shown in Figure 7a,b,c,d. When the absorbance spectrum of the ZnO nanostructure was examined, no significant difference was observed. This can be attributed to the very small nanosize of ZnO nanoparticles [23]. In Figure 7b, the absorbance peak of the Fe_3O_4 nanostructure is recorded as approximately 436 nm. These peaks are consistent with those obtained in the literature [17],[24]. The absorbance peaks of ZnO@Fe_3O_4 nanostructures were detected to be 235 nm, 325 nm, and 380 nm, respectively (Figure 7c-d). Furthermore, optical band gaps of the nanostructures were estimated from Einstein's energy equation (1) [17, 25-27].

$$E_g^{nano} = {hc}/{\lambda} \quad (1)$$

where E_g^{nano} is the energy band gap of the nanoparticles, c is the speed of light, h is Planck's constant, and λ is the cut off wavelength obtained from the absorption spectra. The direct energy band gap of the ZnO nanostructure in Figure 6a was obtained as 2.3 eV. In general, single crystal ZnO band gap is accepted as 3.34 eV. The value obtained in the present study was considerably lower than the value of 3.34 eV. The low values obtained in similar studies in the literature were attributed to the defects in the nanostructure [28]. The optical energy band gap of the Fe_3O_4 nanostructure was found to be 2 eV, which is consistent with the literature [17, 29]. Moreover, as shown in Figure 7c-d, the energy band gap of ZnO@Fe_3O_4 nanostructures was determined around 2.1 eV.

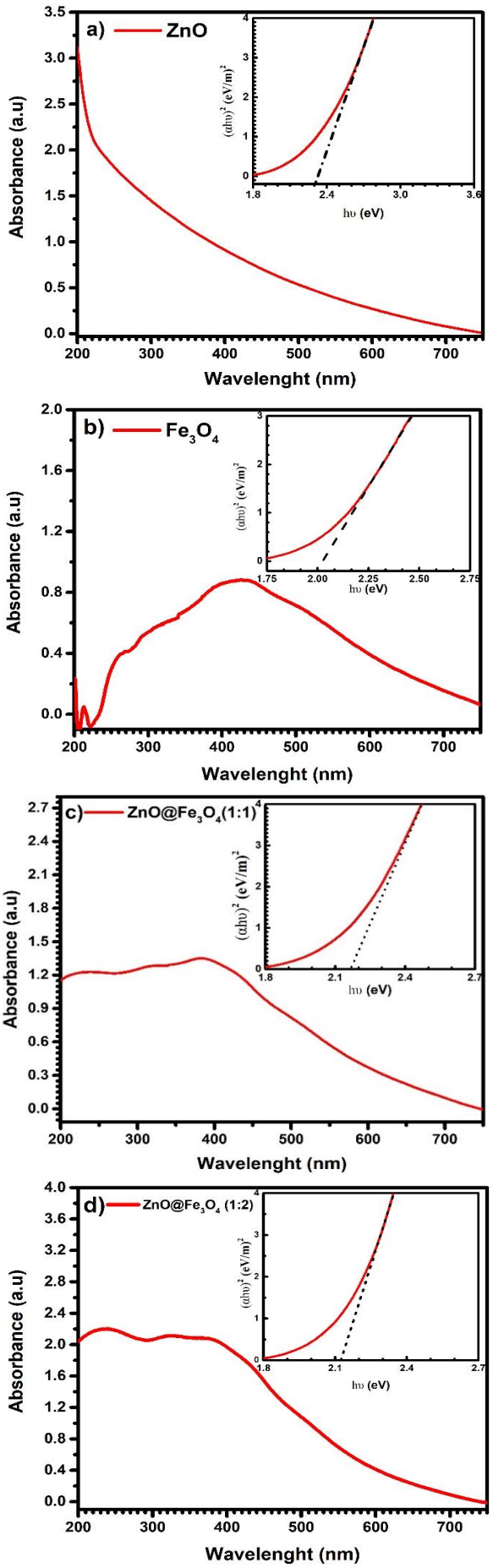

Figure 7. Absorbance and band gap characteristics of ZnO (a), Fe_3O_4 (b), ZnO@Fe_3O_4 -1:1 (c) and ZnO@Fe_3O_4 -1:2 (d) nanostructures

3.3. Magnetic Properties of ZnO@Fe_3O_4 Nanostructures

Magnetic hysteresis curves of ZnO@Fe_3O_4 (1:1) and ZnO@Fe_3O_4 (1:2) nanocomposite structures are shown in Figure 8a and Figure 8b. While the magnetic saturation value of the nanostructure synthesized at a ratio of 1:1 was obtained as 3.76 emu/g, as shown in Figure 8a, that of the nanostructure synthesized at a ratio of 1:2 was obtained as 7.97 emu/g, as shown in Figure 8b. With the doubling of the Fe_3O_4 content by weight ratio, that value approximately doubled as well. However, these values are lower than those found just for the Fe_3O_4 nanostructures in the literature. In their magnetic saturation measurements of Fe_3O_4@Bi2S3 nanoflowers synthesized by the hydrothermal method, Yetim et al., found a value of 89.8 emu/g for the Fe_3O_4 nanostructure [17]. In a similar study, Karacam et al. reported the magnetic saturation values of the Fe_3O_4 nanostructures as 87.7 emu/g and 90.7 emu/g [18]. The magnetic value of the ZnO additive obtained in this study decreased considerably. Sin et al. found the magnetic saturation value as 2.81 emu/g in the ZnO@ Fe_3O_4 nanostructure they synthesized with a facile surfactant-free method [30]. Długosz et al., reported the magnetic saturation value of the Fe_3O_4/ZnO nanostructure they synthesized with a microwave reactor as 9.5 emu/g [22]. This study is consistent with the values obtained in the literature. It is also known that the ZnO structure does not have good magnetic properties. However, it was revealed that a ferromagnetic property was shown through the addition of ZnO to the Fe_3O_4 structure. These results are important especially in terms of the use of ZnO@Fe_3O_4 nanostructures as contrast agents in medical imaging applications [31, 32].

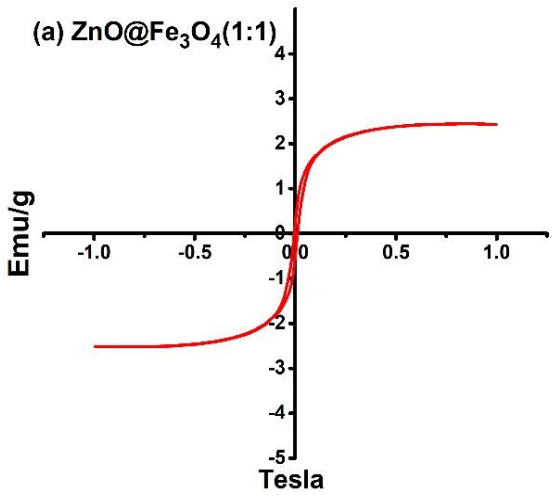

Figure 8. (a) Magnetic hysteresis of ZnO@Fe_3O_4 -1:1 nanostructure

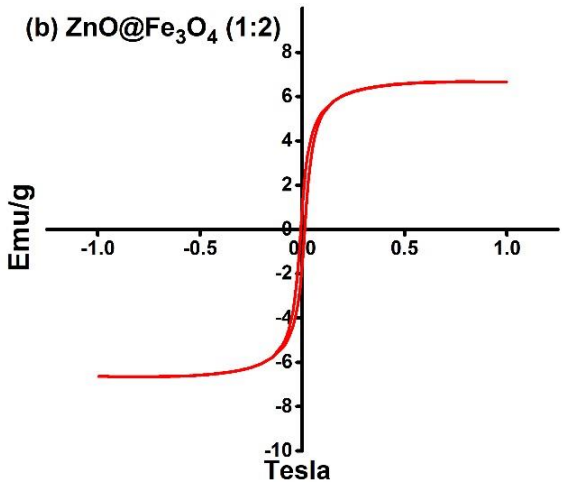

Figure 8. (b) Magnetic hysteresis of ZnO@Fe_3O_4 -1:2 nanostructure

4. CONCLUSIONS

This study investigated the structural, morphological, elemental, optical, and magnetic properties of ZnO@Fe_3O_4 nanostructures synthesized by the hydrothermal method. ZnO@Fe_3O_4 nanostructures were successfully produced by the hydrothermal method. The ZnO and Fe_3O_4 structures were defined in the structural characterization, and no impurity peaks were found. In the morphological images, the presence of composite nanostructures was revealed by both SEM and TEM microscopy. The energy band gaps of the synthesized ZnO@Fe_3O_4 nanostructures were calculated as approximately 2.1 eV. This value is important in terms of being a potential nanomaterial in solar cell, photodetector, photocatalysis, sensor, supercapacitor, and optoelectronic applications, especially with its use in semiconductor technology. In the magnetic susceptibility measurements, the values of 3.76 emu/g and 7.97 emu/g were calculated for ZnO@Fe_3O_4 nanostructures. Although these values show a limited ferromagnetic property, they may contribute to the medical imaging applications of ZnO additive with advanced optical properties.

REFERENCES

[1] Nasrollahzadeh M, Issaabadi Z, Sajjadi M, Sajadi SM, Atarod M. Chapter 2 - Types of Nanostructures. In: Nasrollahzadeh M, Sajadi SM, Sajjadi M, Issaabadi Z, Atarod MBT-IS and T, editors. An Introduction to Green Nanotechnology. Elsevier; 2019. p. 29–80. Available from:https://www.sciencedirect.com/science/article/pii/B978012813586000002X

[2] Pascariu P, Koudoumas E, Dinca V, Rusen L, Suchea MP. Chapter 14 - Applications of metallic nanostructures in biomedical field. In: Dinca V, Suchea MPBT-FNI for E and BA, editors. Micro and Nano Technologies. Elsevier; 2019. p. 341–61. Available from: https://www.sciencedirect.com/science/article/pii/B9780128144015000141

[3] Tripathy N, Kim D-H. Metal oxide modified ZnO nanomaterials for biosensor applications. Nano Converg. 2018;5(1):27. Available from: https://doi.org/10.1186/s40580-018-0159-9

[4] Bahari A, Roeinfard M, Ramzannezhad A. Characteristics of Fe3O4/ZnO nanocomposite as a possible gate dielectric of nanoscale transistors in the field of cyborg. J Mater Sci Mater Electron. 2016;27(9):9363–9. Available from: https://doi.org/10.1007/s10854-016-4978-3

[5] Nurul Ulya H, Taufiq A, Sunaryono. Comparative Structural Properties of Nanosized ZnO/Fe3O4 Composites Prepared by Sonochemical and Sol-Gel Methods. IOP Conf Ser Earth Environ Sci. 2019;276:12059. Available from: http://dx.doi.org/10.1088/1755-1315/276/1/012059

[6] Hong RY, Zhang SZ, Di GQ, Li HZ, Zheng Y, Ding J, et al. Preparation, characterization and application of Fe3O4/ZnO core/shell magnetic nanoparticles. Mater Res Bull. 2008;43(8):2457–68. Available from: https://www.sciencedirect.com/science/article/pii/S0025540807003352

[7] Atla SB, Lin W-R, Chien T-C, Tseng M-J, Shu J-C, Chen C-C, et al. Fabrication of Fe3O4/ZnO magnetite core shell and its application in photocatalysis using sunlight. Mater Chem Phys. 2018;216:380–6. Available from: https://www.sciencedirect.com/science/article/pii/S0254058418305194

[8] Winatapura, D. S., Dewi, S. H., & Adi WA. Synthesis, characterization, and photocatalytic activity of Fe3O4@ZnO nanocomposite. Int J Technol. 2016;7(3):408–16.

[9] Machovsky M, Kuritka I, Kozakova Z. Microwave assisted synthesis of nanostructured Fe3O4/ZnO microparticles. Mater Lett. 2012;86:136–8. Available from: https://www.sciencedirect.com/science/article/pii/S0167577X12010099

[10] Roychowdhury A, Pati SP, Mishra AK, Kumar S, Das D. Magnetically addressable fluorescent Fe3O4/ZnO nanocomposites: Structural, optical and magnetization studies. J Phys Chem Solids. 2013;74(6):811–8. Available from: https://www.sciencedirect.com/science/article/pii/S0022369713000231

[11] Chandekar K V., Shkir M, Khan A, Al-Shehri BM, Hamdy MS, AlFaify S, et al. A facile one-pot flash combustion synthesis of La@ZnO nanoparticles and their characterizations for optoelectronic and photocatalysis applications. J Photochem Photobiol A Chem. 2020;395(3):112465. Available from: https://doi.org/10.1016/j.jphotochem.2020.112465

[12] Senol SD, Ozugurlu E, Arda L. The effect of cobalt and boron on the structural, microstructural, and optoelectronic properties of ZnO nanoparticles. Ceram Int. 2020;46(6):7033–44. Available from: https://doi.org/10.1016/j.ceramint.2019.11.193

[13] Polat S. Production of ZnFe 2 O 4 Doped Carbon Cloth-Based Flexible Composite Electrodes for Supercapacitors. Turk. J. Natur. Sci. 2021;10(2):199–205.

[14] Hasanoğlu Özkan E, Aslan N, Koç MM, Kurnaz Yetim N, Sarı N. Fe3O4 nanoparticle decorated novel magnetic metal oxide microcomposites for the catalytic degradation of 4-nitrophenol for wastewater cleaning applications. J Mater Sci Mater Electron. 2022;33(2):1039–53.

[15] Alula MT, Lemmens P, Madingwane ML. Determination of cysteine via its inhibition of catalytic activity of silver coated ZnO/Fe3O4 composites used for conversion of 4-nitrophenol into 4-aminophenol. Microchem J. 2020;156(2):104976. Available from: https://doi.org/10.1016/j.microc.2020.104976

[16] Kurnaz Yetim N, Kurşun Baysak F, Koç MM, Nartop D. Synthesis and characterization of Au and Bi2O3 decorated Fe3O4@PAMAM dendrimer nanocomposites for medical applications. J Nanostructure Chem. 2021; Available from: https://doi.org/10.1007/s40097-021-00386-w

[17] Kurnaz Yetim N, Aslan N, Koç MM. Structural and catalytic properties of Fe3O4 doped Bi2S3 novel magnetic nanocomposites: p-Nitrophenol case. J Environ Chem Eng. 2020;8(5):104258. Available from:https://www.sciencedirect.com/science/article/pii/S2213343720306072

[18] Karaçam R, Yetim NK, Koç MM. Structural and Magnetic Investigation of Bi2S3@Fe3O4 Nanocomposites for Medical Applications. J Supercond Nov Magn. 2020;33(9):2715–25. Available from: https://doi.org/10.1007/s10948-020-05518-x

[19] Kurnaz Yetim N. Catalytic Properties of Hydrothermally Synthesized Flower-like NiO@Fe3O4. Düzce Univ J Sci Technol. 2020;(8):1964–74.

[20] Bahtiar S, Taufiq A, Utomo J, Hidayat N, Sunaryono. Structural Characterizations of Magnetite/Zinc Oxide Nanocomposites Prepared by Co-precipitation Method. IOP Conf Ser Mater Sci Eng. 2019;515:12076. Available from: http://dx.doi.org/10.1088/1757-899X/515/1/012076

[21] Siregar J, Sebayang K, Yuliarto B, Humaidi S. XRD characterization of Fe3O4-ZnO nanocomposite material by the hydrothermal method. AIP Conf Proc. 2020;2221(3):1–5.

[22] Długosz O, Szostak K, Krupiński M, Banach M. Synthesis of Fe3O4/ZnO nanoparticles and their application for the photodegradation of anionic and cationic dyes. Int J Environ Sci Technol. 2021;18(3):561–74. Available from: https://doi.org/10.1007/s13762-020-02852-4

[23] Goh EG, Xu X, McCormick PG. Effect of particle size on the UV absorbance of zinc oxide nanoparticles. Scr Mater. 2014;78–79:49–52. Available from: https://www.sciencedirect.com/science/article/pii/S1359646214000372

[24] Wang X, Chen X, Gao L, Zheng H, Zhang Z, Qian Y. One-Dimensional Arrays of Co3O4 Nanoparticles: Synthesis, Characterization, and Optical and Electrochemical Properties. J Phys Chem B. 2004 Oct 1;108(42):16401–4. Available from: https://doi.org/10.1021/jp048016p

[25] Bhadwal AS, Tripathi RM, Gupta RK, Kumar N, Singh RP, Shrivastav A. Biogenic synthesis and photocatalytic activity of CdS nanoparticles. RSC Adv. 2014;4(19):9484–90. Available from: http://dx.doi.org/10.1039/C3RA46221H

[26] Yetim NK, Aslan N, Sarıoğlu A, Sarı N, Koç MM. Structural, electrochemical and optical properties of hydrothermally synthesized transition metal oxide (Co3O4, NiO, CuO) nanoflowers. J Mater Sci Mater Electron. 2020;31(15):12238–48. Available from: https://doi.org/10.1007/s10854-020-03769-x

[27] Yetim NK, Kurş F. Magnetic and Structural Characterization of Inorganic/Organic coated. J Mater Electron Devices. 2021;2:12–8.

[28] Hu Y, Chen H-J. Preparation and characterization of nanocrystalline ZnO particles from a hydrothermal process. J Nanoparticle Res. 2008;10(3):401–7. Available from: https://doi.org/10.1007/s11051-007-9264-0

[29] Kulkarni SA, Sawadh PS, Palei PK, Kokate KK. Effect of synthesis route on the structural, optical and magnetic properties of Fe3O4 nanoparticles. Ceram Int. 2014;40(1, Part B):1945–9. Available from:https://www.sciencedirect.com/science/article/pii/S0272884213008973

[30] Sin J-C, Tan S-Q, Quek J-A, Lam S-M, Mohamed AR. Facile fabrication of hierarchical porous ZnO/Fe3O4 composites with enhanced magnetic, photocatalytic and antibacterial properties. Mater Lett. 2018;228:207–11. Available from: https://www.sciencedirect.com/science/article/pii/S0167577X18309340

[31] Koç MM, Aslan N, Kao AP, Barber AH. Evaluation of X-ray tomography contrast agents: A review of production, protocols, and biological applications. Microsc Res Tech. 2019;82(6):812–48.

[32] Aslan N, Ceylan B, Koç MM, Findik F. Metallic nanoparticles as X-Ray computed tomography (CT) contrast agents: A review. J Mol Struct. 2020;1219:128599. Available from: https://www.sciencedirect.com/science/article/pii/S0022286020309248